Controlled release of Rituximab from gold nanoparticles for phototherapy of malignant cells

ARTICLE *in* JOURNAL OF CONTROLLED RELEASE · JUNE 2012

Impact Factor: 7.71 · DOI: 10.1016/j.jconrel.2012.06.030 · Source: PubMed

4 AUTHORS, INCLUDING:

Gili Bisker
Massachusetts Institute of Technology
17 PUBLICATIONS **176** CITATIONS
SEE PROFILE

Daniella Hayon
Technion - Israel Institute of Technology
14 PUBLICATIONS **205** CITATIONS
SEE PROFILE

Journal of Controlled Release 162 (2012) 303–309

Contents lists available at SciVerse ScienceDirect

Journal of Controlled Release

journal homepage: www.elsevier.com/locate/jconrel

Controlled release of Rituximab from gold nanoparticles for phototherapy of malignant cells

Gili Bisker, Daniella Yeheskely-Hayon, Limor Minai, Dvir Yelin *

Department of Biomedical Engineering, Technion-Israel Institute of Technology, Haifa 32000, Israel

ARTICLE INFO

Article history:
Received 6 May 2012
Accepted 22 June 2012
Available online 1 July 2012

Keywords:
Rituximab
Gold nanoparticles
Femtosecond pulses
Plasmon resonance
Complement dependent cytotoxicity
Controlled drug release

ABSTRACT

Releasing drug molecules at their targets with high spatial and temporal accuracy could aid numerous clinical applications which require low systemic damage and low side effects. Nano-carriers of drugs are an attractive solution for such task, allowing specific accumulation in tumors and gradual release of their payload. Here, we utilize gold nanospheres conjugated to Rituximab, an anti-CD20 monoclonal antibody-based drug, for carrying and releasing the drug upon irradiation of specifically tailored femtosecond laser pulses. The released anti-CD20 molecules retain their functionality and ability of triggering the complement-dependent cytotoxicity. This effect comes in addition to cell necrosis caused by the plasmonic nanometric shock waves emanating from the nanospheres and rupturing the plasma membranes. Main advantages of the presented technique include high spatial and temporal resolution, low toxicity and high repeatability and consistency due to the morphological stability of the nanospheres.

1. Introduction

Controlling drug release at specific locations within the body is an important challenge in cancer therapy, allowing efficient delivery which reduces the minimal drug dosage and avoids undesirable side effects. Nanotechnology has yielded numerous drug carriers on a nanometric scale, some of which are already clinically approved for *in-vivo* applications [1–4] including polymers [5], dendrimers [6], liposomes [7,8], micelles [9], peptides [10], and nanogels [11]. Various mechanisms have been demonstrated useful for releasing the drugs from their carriers, including electrical stimulation [12], external magnetic field [13], acidic pH environment [14] and ultrasound waves [15]. Using light in the visible and near-infrared range is particularly attractive for triggering [16] and releasing drugs [17] due to potentially high specificity and low overall toxicity. Optically triggered release was demonstrated using several light sensitive substances including silica nanoparticles [18] and block-copolymer micelle nano-carriers [19].

The unique optical and chemical properties of gold nanoparticles [20] make them excellent potential candidates for carrying and releasing drugs under external optical signals. Liposomes loaded with gold nanoparticles had released their molecular content upon UV light [21], nanosecond-pulse laser irradiation [22] and near-infrared femtosecond pulses [23]. Capsules combining metal nanoparticles released their encapsulated fluorescent polymers when illuminated with near-infrared laser due to local temperature rise [24,25]. Gold nanoparticles were also proven effective as nano-carriers for drug delivery application [26,27] owing to straight-forward synthesis methods [28], high biocompatibility [28,29] and tendency to accumulate in cancerous tissues by the enhanced permeability and retention (EPR) effect [30–32]. Gold nanocages with porous walls coated by a temperature sensitive polymer were used as drug carriers which release their effectors following near-infrared irradiation [33]. UV irradiation was used to break photo-cleavable bonds, releasing 5-fluorouracil molecules from gold nanoparticle [34] and regulating in-cell release of DNA molecules [35]. Using optical wavelengths tuned to the plasmonic resonance of the gold nanoparticles was shown useful for detaching molecules from their surfaces [26] and for removing their coating molecular layer by breaking the gold-sulfur bond [36,37]. Optical pulses having duration shorter than the characteristic heat diffusion time constant from a gold nanoparticle (approximately 6 ps [38,39]) are considerably more efficient in delivering the optical energy into the particles, allowing nanometer-scale thermal and chemical effects and reducing collateral tissue damage [40–44].

The interaction between laser light and gold nanoparticles could also be utilized for specifically damaging cancerous cells [45,46] and tissue [47–49]. Branched gold nanoparticles specifically attached to breast and ovarian cancer cells have been shown to destroy their target cells upon visible continuous wave (CW) laser irradiation [50]. CW lasers have also been used for photothermal therapy of carcinoma cells targeted by gold nanoparticles [51–53], and of breast cancer cells internalizing capsules containing metal nanoparticles [54]. Recently, short pulse lasers have been shown to be more effective than CW lasers in inducing necrosis in nanoparticle-conjugated cells [55]. Nanosecond and picosecond pulses were utilized for thermolysis of leukemia cells with clusters of gold nanoparticles [56] and of breast cancer cells targeted by gold nanocages [57,58]. Pulses in the femtosecond range, which in some conditions may induce multiphoton ionization in

* Corresponding author. Tel: +972 4 8293832; fax: +972 4 8294599.
E-mail address: yelin@bm.technion.ac.il (D. Yelin).

0168-3659/$ – see front matter © 2012 Elsevier B.V. All rights reserved.
doi:10.1016/j.jconrel.2012.06.030

addition to rapid heating [44], were reported effective in damaging cancerous HeLa cells conjugated to gold nanorods [59]. Recently, our group has shown that single resonant femtosecond laser pulses in the visible wavelength range may induce well-controlled necrosis, apoptosis and fusion of epidermoid carcinoma cells and Burkitt lymphoma cells targeted by antibody-coated gold nanospheres [60].

A hybrid approach for both photothermal therapy and local photo-induced drug release was recently demonstrated using gold nanoshells encapsulating doxorubicin [61,62]. A particularly attractive approach for such hybrid therapy would be to utilize an antibody-based cancer drug [63] which would be useful both for specific targeting and for promoting necrosis through the patients' own complement-dependent cytotoxicity (CDC) system. To date, only a few antibodies are approved for therapy, including Trastuzumab (Herceptin®) [64], Bevacizumab (Avastin®) [65], Cetuximab (Erbitux®) [66] and Rituximab (Rituxan®) [67]. The Rituximab monoclonal antibody has been recently shown successful in binding CD20 receptors on B-cells and promoting cell death in three distinct mechanisms: cell necrosis through the CDC system [68,69], cell necrosis through antibody-dependent cellular cytotoxicity (ADCC) [68] and cell apoptosis [70].

In this work, we demonstrate the feasibility of controlled release of Rituximab from gold nanospheres using resonant irradiation of femtosecond pulses. When targeted to malignant B-cells the gold nanosphere-Rituximab conjugates are found to induce cell necrosis in two independent and complimentary paths; one through direct rapture of the plasma membrane and the other via the CDC mechanism. The dual roles of both the nanospheres (as drug carriers and phototherapy mediators) and of the antibodies (as targeting agents and activators of the CDC mechanism) is quantified by measuring the amount and functionality of the released antibody, and demonstrated by studying light-induced necrosis in cells targeted by the nano-conjugates.

2. Materials and methods

2.1. Nanoparticles-anti-CD20 preparation

Gold nanospheres were prepared using a well-known citrate reduction protocol [71,72], yielding approximately 0.1 nM of 20-nm-diameter citrate-capped gold spheres. Coating the nanoparticles by chimeric anti-CD20 monoclonal antibody (Rituximab) was obtained by mixing 10 mg/ml Rituximab and 0.082 mg/ml NHS-Polyethylene glycol-OPSS (NHS-PEG-OPSS, 3.4 kDa, Creative PEGWorks, USA) with 1:1.4 molar ratio in 100 mM sodium bicarbonate buffer at pH 8.5 for overnight stirring [60,73]. The citrate-capped gold nanoparticles were then added to the anti-CD20-PEG solution in a 1:1 volume ratio for additional overnight incubation. The anti-CD20 molecules were conjugated to the gold nanoparticles by thiol-gold bonds via the NHS-PEG-OPSS cross-linker, replacing the citrate capping. The resulting anti-CD20-coated gold nanoparticles were washed five times with phosphate buffered saline (PBS), centrifuged and 10-fold concentrated to 1 nM in PBS. The functionalized gold nanoparticles were stored at 4 °C, and remained well dispersed and stable for over a month. Laser irradiation and spectroscopy measurements were conducted while the nanoparticle solution was placed within the 0.75-mm gap between two microscope slides which were placed on a motorized stage of an inverted optical microscope.

2.2. Laser irradiation

For irradiating the nanoparticle–antibody conjugates at their resonance wavelength, a Ti:sapphire oscillator-amplifier system was used with an additional optical parametric amplifier, producing approximately 50 fs pulses at 545 nm wavelength and 1 kHz repetition rate (Newport Corp.). Beam intensity was controlled using variable neutral density filters. The pulse train was directed through one of the ports of the microscope and was slowly focused by a long (500 mm) focal length lens, yielding a 300 μm spot on the sample plane which was positioned 25 mm from the focal plane. The sample was scanned using two scanning mirrors at average speed of 44 mm/s on the sample, producing a repetitive single pulse illumination every 44 μm, corresponding to approximately 40 pulses per each sample location. Extinction spectrum of the irradiated samples was measured in real-time using a tungsten-halogen lamp and a spectrometer placed in one of the microscope's ports.

2.3. Gel electrophoresis and western blot

After irradiation, the nanoparticle–antibody solution was analyzed using 12% Tris-Glycine sodium dodecyl sulfate polyacrylamide gel electrophoresis (SDS-PAGE) system and coomassie staining. Higher detection sensitivity and specificity were obtained using western blot analysis, at which the anti-CD20 molecules were transferred from the gel to polyvinylidene fluoride (PVDF) membrane. Anti-CD20 bands were labeled using horseradish peroxidase (HRP) conjugated goat anti-human secondary antibody and visualized using luminescent image analysis system (Fujifilm LAS-3000).

2.4. Cell line

Human CD20-positive B-cell line (BJAB-Burkitt lymphoma cell line of approximately 1.6×10^5 CD20 receptors per cell [74]) were grown in RPMI-1640 medium supplemented with 10% heat-inactivated fetal bovine serum, 2 mM glutamine and 5 mM sodium pyruvate. Cells were grown in a 5% CO_2 atmosphere in a 37 °C fully humidified incubator and were maintained at concentrations bellow 10^6 cells/ml to ensure logarithmic growth.

2.5. Anti-CD20 – B-cells binding assay

The ability of the released anti-CD20 molecules to bind to CD20-expressing cells was evaluated by incubating 6 μl of 31-fold concentrated supernatants of irradiated particles with approximately 7.5×10^4 cells for 30 min at room temperature, followed by three PBS washes. FITC-conjugated mouse anti-human secondary antibody was added to the samples at 1:500 dilution ratio, followed by 30 min incubation at 4 °C, three subsequent washes with PBS and resuspension in fresh medium. The fluorescence signal from the FITC conjugates was quantified using fluorescence activated cell sorting (BD FACS Calibur).

2.6. Complement dependent cytotoxicity (CDC) assay

To assess the cytotoxicity triggered by the released antibodies, 5×10^5 Burkitt lymphoma (BJAB) cells/ml were suspended in PBS with 1 mM $CaCl_2$, 1 mM $MgCl_2$ and 2 μg/μl Propidium iodide (PI). 30 μl of 18-fold concentrated supernatants of irradiated anti-CD20 coated gold nanoparticles was added to the 100 μl cell medium. Samples were incubated for 15 min at 37 °C followed by addition of 130 μl of either active or heat-inactivated (56 °C, 30 min) human serum for additional incubation of 4 h at 37 °C. Quantification of BJAB cells necrosis was carried out using FACS.

2.7. Cell irradiation

After verifying the cytotoxicity of the CD20 antibodies which were dissociated from the nanoparticles, the pulse irradiation experiment was repeated in the presence of the BJAB cells which were incubated with different concentrations of Rituximab-coated gold nanoparticles for 20 min prior to the laser treatment. Necrosis labeling was obtained by suspending 5×10^5 BJAB cells/ml in PBS with 1 mM $CaCl_2$, 1 mM $MgCl_2$ and 2 μg/μl Propidium iodide. The cells were cultured in a multi-well plate (Lab-TekII, Nunc., 100 μl per well) which was placed on top of the

microscope's motorized stage within a compact incubator in controlled temperature (37 °C) and CO_2 concentration (Okolab Inc.). CDC was tested 15 min after irradiation as describe above.

3. Results

3.1. Controlled release of anti-CD20 molecules from gold nanoparticles

In order to demonstrate and quantify the pulse-activated release of Rituximab from its gold nanoparticle carriers, the antibody molecules were conjugated to the nanoparticles in a ratio of approximately 200 molecules per particle (estimated using SDS-PAGE band intensity analysis, see supplementary Fig. S1). The solution of the anti-CD20-nanoparticle conjugates was irradiated by a femtosecond pulse train whose wavelength was tuned to match the nanoparticles' plasmonic resonance (Fig. 1a).

Following irradiation, the measured extinction spectra showed noticeable red shift and loss of the plasmonic resonance peak with increasing pulse fluence values (Fig. 1b), an indication of particle aggregation [75,76] and possible alteration of their antibody coating layers [28,77], most probably due to S–Au bond breakage [36,40–43]. Western blot analysis of the extracted supernatant solution (Fig. 2) has confirmed the release of the anti-CD20 molecules from the gold nanoparticles (Fig. 2, lanes b–d), showing clear bands at the characteristic molecular weights of the light and heavy chains of the antibody. Prior to laser irradiation no free Rituximab molecules were found in the nanoparticle solution (Fig. 2, lane a).

By comparing the band intensities corresponding to the light molecular chain of the antibody between supernatants of irradiated conjugates and free Rituximab of known concentrations, we estimate release efficiency of up to 3% of the bound molecules into the medium (supplementary Fig. S2).

3.2. Binding of released Rituximab molecules to BJAB cells

The ability of the released anti-CD20 molecules to bind to CD20 receptors on human B-cells was demonstrated by incubating BJAB cells with supernatants from irradiated samples of anti-CD20-nanoparticle conjugates and detecting the antibody-receptor binding using a FITC-conjugated anti-human secondary antibody (Fig. 3). Cells incubated with an irradiated nanoparticles supernatant solution showed noticeably higher fluorescence (Fig. 3a) compared to cells incubated with a non-irradiated solution (Fig. 3b), confirming that antibodies were released from the nanoparticles and had retained their ability to bind to CD20 receptors on the cells' plasma membranes. The strong fluorescence signals were roughly similar to those obtained following incubation with a pure 0.1 μg Rituximab sample (Fig. 3c). A control image of cells incubated with only the secondary antibody showed very low fluorescence signals due to some nonspecific binding (Fig. 3d).

Histograms of cell fluorescence intensity showed (Fig. 3e) high percentage (approximately 80%) of cells having high fluorescence signals following incubation with irradiated nanoparticles (cyan curve), similar to cells which were incubated with 0.01 μg Rituximab (red curve, no nanoparticles, no irradiation) but significantly more than the control cells (blue curve) or cells which were incubated with non-irradiated nanoparticles (green curve), confirming that the released antibodies were indeed efficiently binding to the CD20 rec-eptors. Additional control sample containing cells without the FITC conjugated secondary antibody showed weak auto-fluorescence background (black curve).

3.3. Complement dependent cytotoxicity of released Rituximab

One of the most significant mechanisms in which Rituximab promotes cell death is through complement dependent cytotoxicity, where complement proteins in the blood serum act to induce necrosis of cells marked by Rituximab [78]. Following laser irradiation (40 pulses,

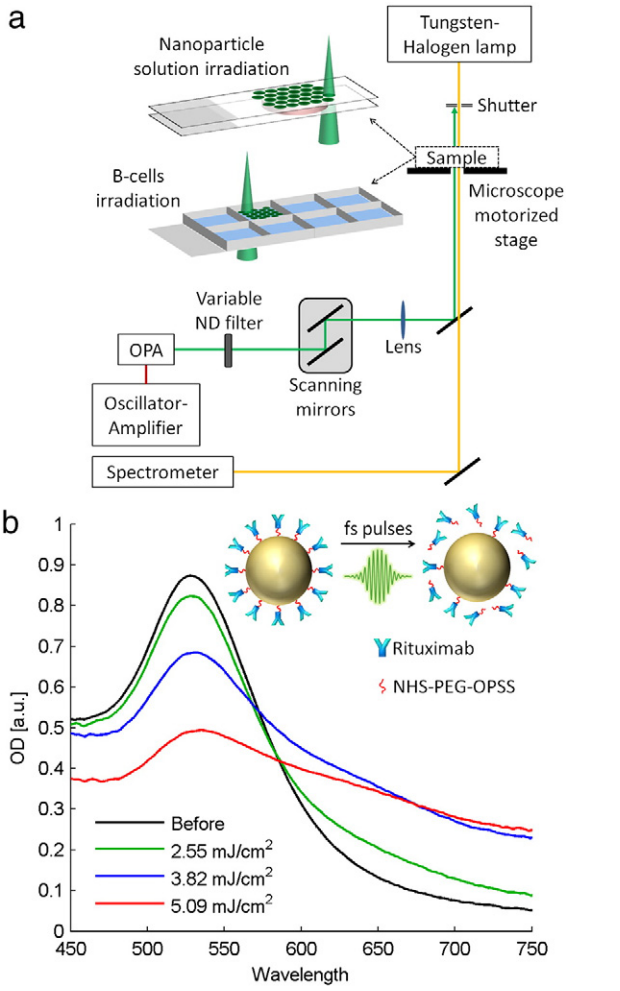

Fig. 1. (a) Optical setup for controlled release of Rituximab molecules from gold nanoparticles. ND – neutral density. OPA – optical parametric amplifier. (b) Extinction spectra of Rituximab-coated gold nanoparticles before (black curve) and after irradiation of approximately 40 pulses of 2.55 mJ/cm^2 (green curve), 3.82 mJ/cm^2 (blue curve), and 5.09 mJ/cm^2 (red curve) per pulse.

3.82 mJ/cm^2 per pulse) of the anti-CD20-nanoparticle conjugates, the released antibodies were added to the BJAB cells growth medium together with an active blood serum which contained all the necessary components of the CDC system. Compared to control cells and cells incubated with non-irradiated nanoparticles which showed approximately 6% necrosis (Fig. 4a,b), extensive 21% necrosis was measured in cells incubated with irradiated nanoparticles (Fig. 4c), indicating that the released Rituximab molecules were binding to the cells and have triggered the CDC. Comparable necrosis levels of 16.5% and 35.4% were obtained by adding 1 μg (Fig. 4d) and 10 μg (Fig. 4e) Rituximab to the cells medium, respectively. The FACS measurements are summarized in a bar chart in Fig. 4f, revealing that the CDC effect on the cells resulting from the released antibody was equivalent to that induced by a few μg of Rituximab, which corresponds to approximately 10^3–10^4 Rituximab molecules (within the 100 μl sample volume) per single CD20 receptor.

3.4. Combined effects of photothermal therapy and complement dependent cytotoxicity

When cells are targeted by gold nanoparticles and irradiated by intense laser pulses, the resulting pulse–particles interactions could initiate cell death, irrespective of the released molecules from the particles' surfaces; such effect is well known as photothermal therapy, and has been extensively studied [47]. Photo-induced therapy has also been

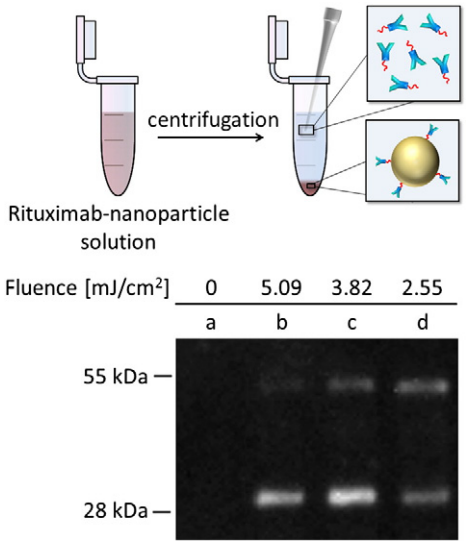

Fig. 2. (a) Extraction of the released antibodies from the irradiated nanoparticles. (b) Western blot analysis of the supernatant of Rituximab-coated gold nanoparticles solution before irradiation (lane a) and following laser irradiation of 40 pulses of 5.09 mJ/cm^2 (lane b), 3.82 mJ/cm^2 (lane c), and 2.55 mJ/cm^2 (lane d) per pulse.

studied by our group [60] using irradiation parameters (50 fs pulses, 550 nm wavelength) similar to those used in this work to release the antibodies from the nanoparticles, to demonstrate specific cell necrosis in irradiated BJAB cells targeted by anti-CD20 - gold nanoparticle conjugates. In order to demonstrate photo-induced therapy combined with triggered local cytotoxicity induced by released antibodies, BJAB cells were incubated with Rituximab-coated gold nanoparticles and irradiated by a train of resonant pulses (40 pulses, 3.82 mJ/cm^2 per pulse). Following the addition of active serum which contained all necessary components for inducing CDC, the irradiated cells showed noticeably higher necrosis levels (Fig. 5, upper raw) compared to irradiated cells incubated with heat-inactivated serum (Fig. 5, lower row), indicating that the CDC mechanism was responsible for the additional cell death over that induced by the photothermal effect alone [60]. Note that irradiated cells without nanoparticles remained viable (Fig. 5, leftmost columns), indicating that laser irradiation alone had no toxic effect on the cells. Non-irradiated control cells to which neither active nor inactive serum was added remained viable (data not shown), implying that Rituximab molecules that were still attached to the gold nanoparticles did not activate the CDC mechanism.

A bar chart summarizing the percentage of necrotic cells relative to control cells without nanoparticles, for different particle concentrations, reveals (Fig. 6) statistically significant ($P<0.0001$) higher level of necrosis of irradiated cells (blue bars) compared to irradiated cells suspended in heat-inactivated serum (red bars), while more than 96% of the non-irradiated cells have remained viable for all particle concentrations (green bars).

4. Discussion

Gold nanoparticles functionalized by drug molecules which also have high affinity for certain targeted cells or tissue can serve both as drug carriers and photo-damage mediators for a single therapeutic task. In this work we have demonstrated that gold nanoparticles conjugated with Rituximab, an FDA approved drug for treatment of various hematological malignancies and autoimmune diseases, are able to bind to their target cells and release their load upon irradiation by specifically tailored sequence of ultrashort laser pulses, while at the same time, affect their target cells through an additional, com-plementary mechanism of photo-induced membrane rupture [60]. We show that resonant femtosecond pulses cause release of

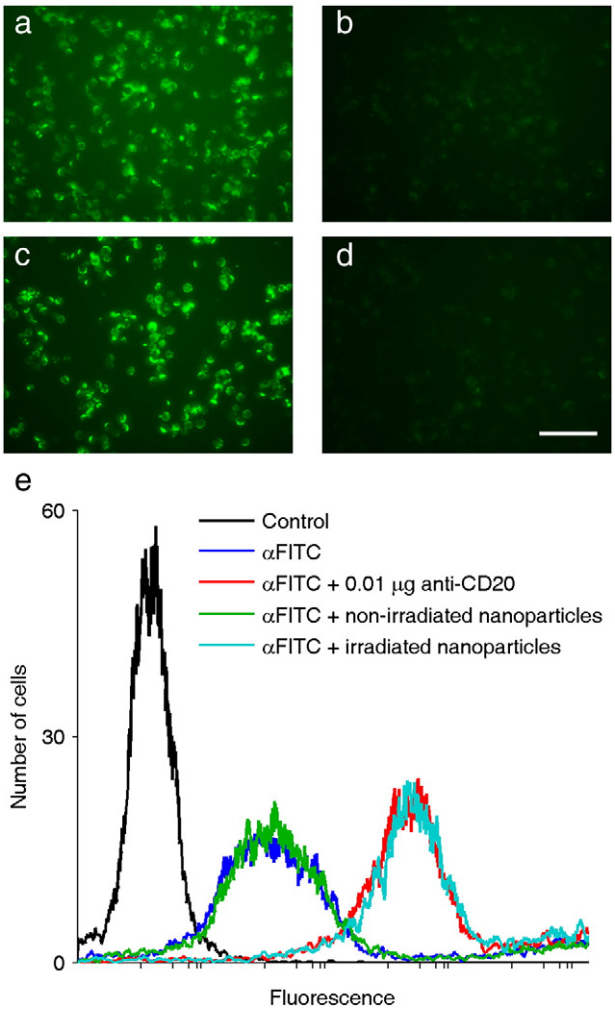

Fig. 3. Affinity of the released drug molecules to CD20 receptors on BJAB cellsmembranes. (a) Cells incubated with released anti-CD20 from irradiated gold nanoparticles. (b) Cells incubated with supernatant form non-irradiated nanoparticles. (c) Cells incubated with free 0.1 μg Rituximab. (d) Control cells with the secondary antibody. Scale bar represents 100 μm. (e) Cell number histograms as a function of fluorescence (logarithmic scale) of BJAB cells only (black curve), cells with secondary antibody (blue curve), cells with 0.01 μg Rituximab and secondary antibody (red curve), cells with supernatant from non-irradiated nanoparticles and secondary antibody (green curve), and cells with released anti-CD20 from irradiated nanoparticles and secondary antibody (cyan curve). The similarity between the histograms of cells with the light-released antibody and with the pure antibody samples (cyan and red curves, respectively) proves the high affinity of the released drug to CD20 receptors. Each histogram includes approximately 5×10^3 cells. αFITC – anti human FITC conjugated secondary antibody.

Rituximab molecules from the surface of gold nanoparticles at rates of approximately six antibody molecules per particle per 40 pulses, sufficient for the induction of cell necrosis via CDC. The exact mechanism underlining the release of the Rituximab is not fully understood and may involve thermal and mechanical effects, as well as cleavage of the thiol bond between the PEG cross-linker and the gold surface [36,40–43] which may result from the coupling between excited electrons in the gold particles and the S–Au vibration modes [43]. The effect of the drug release cannot be easily decoupled, however, from the mechanical or photo-chemical effect induced by the cavitation bubble formed around the nanoparticles [79], compromising membrane integrity and reducing cell viability. In fact, since the drug release and the cavitation bubbles are initiated at roughly similar irradiation parameters, further research would be required in an attempt to better control each process separately, or for improving the synergy between them for attaining a desirable cellular damage.

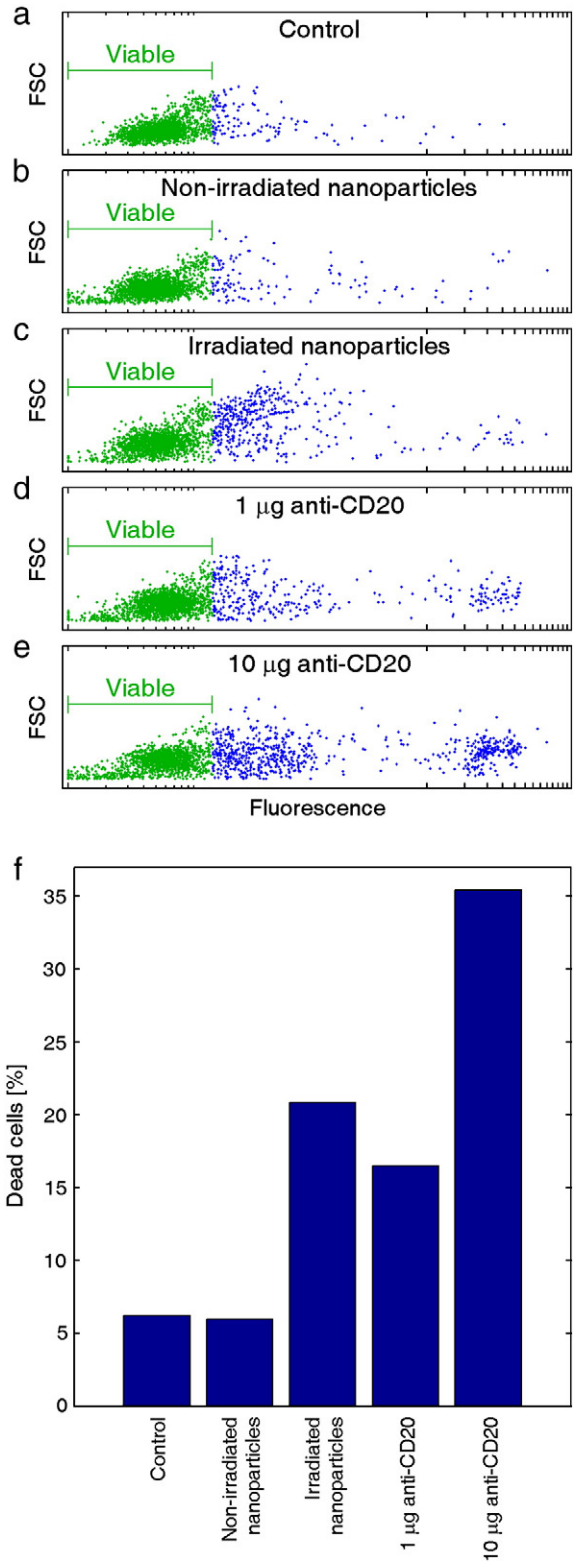

Fig. 4. Efficacy of the released drug molecules in the presence of CDC-active serum. (a) A dot plot of the forward scattering (FSC) signal against the Propidium iodide fluorescence (logarithmic scale) for quantification of necrotic BJAB cells in the presence of active blood serum. (b) Same as (a), with the addition of supernatants of non-irradiated anti-CD20-nanoparticle conjugates. (c) Same as (a), with the addition of released antibody from irradiated anti-CD20-nanoparticle conjugates. (d) Same as (a), with the addition of 1 μg Rituximab. (e) Same as (a) with the addition of 10 μg Rituximab. Green dots represent viable cells; Blue dots represent dead cells. Each plot accounts for 2×10^3 cells. (f) Bar chart showing the percentage of dead cells for each experiment (a–e).

An important benefit of the hybrid approach presented in this work is the high temporal and spatial control over the release process: the strong chemical bonds between the drug and the gold nanospheres prevent nonspecific release of the drug in regions which are not irradiated by the pulse laser, allowing precise timing of the release on the femtosecond time scale and high localization determined by the nanoparticle attachment sites (nanometer scale) and the laser irradiation spot (micron scale). Moreover, the high structural stability of the gold nanospheres under intense pulse irradiation compared, for example, to nanorods [80] and nanoshells [81] permits the use of additional irradiation doses which would still be effective in inducing photothermal and photochemical effects which may cause degradation [82,83] or denaturation [84] of nearby biological molecules, enhancing the desired therapeutic effect to the tissue. The main weakness of using gold nanospheres is the limited penetration depth of their resonance wavelength into thick scattering tissue. Compared with near infrared wavelengths, the high scattering in the visible range may increase the required light intensity illuminating the tissue and broaden the effective pulse duration reaching particles deep below the surface.

Some technical issues would still need to be addressed in further research in order to refine the drug release method and improve its efficiency. For example, one question which needs to be studied is the mutual competition between the antibody-coated nanoparticles and the released free antibody molecules on available CD20 receptors on the cell membrane. While low nanoparticle concentrations may not suffice for efficient CDC activation, high concentrations could leave no free CD20 receptors for binding the released antibodies. Such competition would not be an issue, though, in cases where the irradiation causes the nanospheres to detach from an antibody that is already attached to a receptor. In such case, the remained antibody would be available for interacting with the CDC proteins to promote cell death. Improved efficiency of the CDC activation could also be gained by choosing a cross-linker molecule that does not interfere with the initiation of the complementary cytotoxicity cascade. Since the pulse-laser irradiation results in the cleavage of the gold-sulfur bond between the particle and the cross-linker thiol end, the released antibody may remain attached to the linker molecule through one of its side chains, which may inhibit the complementary proteins from recognizing their binding site. A more sophisticated cross-linker with a customized functional group aimed for a free binding site on the antibody could increase the efficiency of the cytotoxicity mechanism induced by the released drug. Finally, in contrast to encapsulating carriers [7,54] which can carry large payloads to their targets, our gold nanospheres carry the molecules only on their (outer) surface; larger particles would be able to carry more drug and would also require lower fluence values for the cleavage of S–Au bonds [37] due to higher absorption and near-field efficiencies [44].

5. Conclusion

The controlled release of an anti-cancer drug Rituximab is demonstrated with high specificity and efficiency sufficient for initiating cell death through the CDC system in lymphoma B-cells. Using a femtosecond pulsed laser whose wavelength is tuned to the plasmonic resonance of the gold nanoparticle carriers, we have demonstrated the release of the drug molecules into the medium, verified their binding ability to their corresponding cell receptors, showed their ability to trigger a cascade of CDC, and finally, demonstrated this technique together with the induction of cellular photo-damage caused by direct interaction between the nanospheres and the cells. The proof of concept presented here could be conducted using other antibodies, specific drugs or other biomolecules of interest, utilizing the plasmonic shockwave effect which occurs upon resonant irradiation of the gold nanospheres carriers. With or without the accompanied photothermal effect, this technique could provide a valuable tool for treating various diseases at high precision and with minimal toxicity.

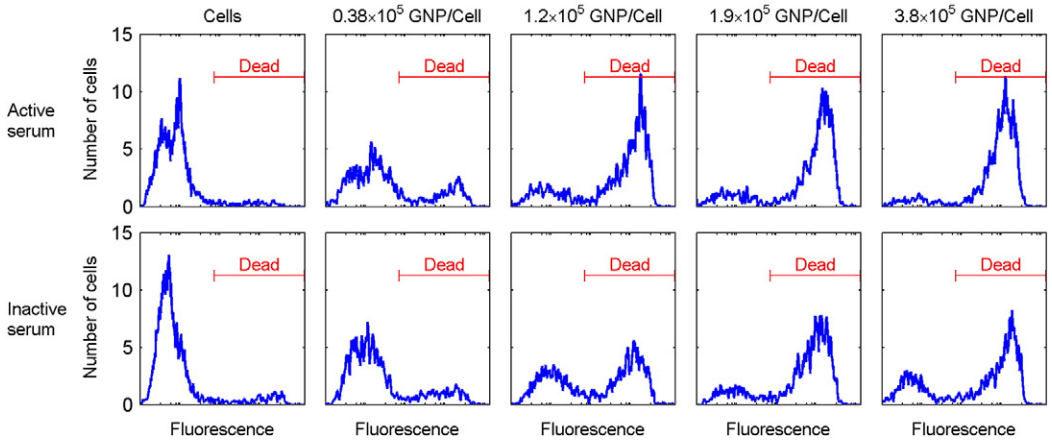

Fig. 5. Necrosis in irradiated cells targeted by different concentrations of anti-CD20 – gold nanoparticle conjugates. The regions of high fluorescence signals marked by the red lines indicate dead necrotic cells. The horizontal axes have logarithmic scales and their units are arbitrary. Each histogram accounts for more than 1.4×10^3 cells. GNP – gold nanoparticles.

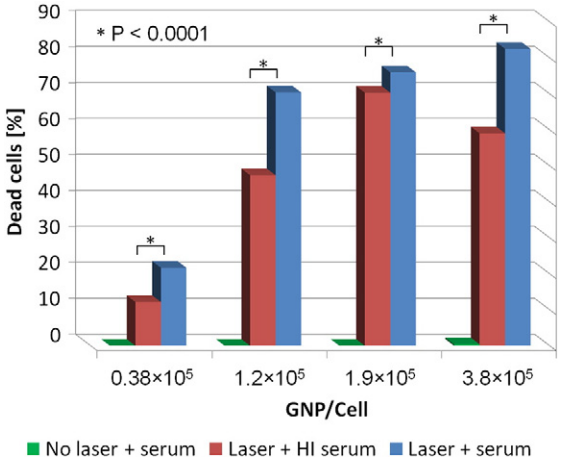

Fig. 6. Quantification of necrotic BJAB cells following laser irradiation with active serum (blue), inactive-serum (red) serum, and with no laser irradiation (green). GNP – gold nanoparticles. HI – heat inactivated.

Acknowledgments

The authors thank Prof. Doron Melamed for providing the Burkitt lymphoma cell line, Prof. Eldad J. Dann for valuable discussions, and Lior Golan for his technical assistance. This work was funded in part by the European Research Council starting grant (239986) and by the Lorry I. Lokey Interdisciplinary Center for Life Sciences and Engineering.

Appendix A. Supplementary data

Supplementary data to this article can be found online at http://dx.doi.org/10.1016/j.jconrel.2012.06.030.

References

[1] D. Peer, J.M. Karp, S. Hong, O.C. Farokhzad, R. Margalit, R. Langer, Nanocarriers as an emerging platform for cancer therapy, Nat. Nanotechnol. 2 (2007) 751–760.
[2] M.E. Davis, Z. Chen, D.M. Shin, Nanoparticle therapeutics: an emerging treatment modality for cancer, Nat. Rev. Drug Discov. 7 (2008) 771–782.
[3] J.B. Wolinsky, Y.L. Colson, M.W. Grinstaff, Local drug delivery strategies for cancer treatment: gels, nanoparticles, polymeric films, rods, and wafers, J. Control. Release 159 (2012) 14–26.
[4] K. Park, Nano is better than micro for targeted vaccine delivery, J. Control. Release 144 (2010) 117.
[5] S. Moein Moghimi, Recent developments in polymeric nanoparticle engineering and their applications in experimental and clinical oncology, Anticancer Agents Med. Chem. 6 (2006) 553–561 (Formerly Current Medicinal Chemistry - Anti-Cancer Agents).
[6] C.M. Paleos, D. Tsiourvas, Z. Sideratou, L. Tziveleka, Acid- and salt-triggered multifunctional poly(propylene imine) dendrimer as a prospective drug delivery system, Biomacromolecules 5 (2004) 524–529.
[7] G. Blume, G. Cevc, Liposomes for the sustained drug release *in vivo*, Biochim. Biophys. Acta - Biomembranes 1029 (1990) 91–97.
[8] W.C. Zamboni, Liposomal, nanoparticle, and conjugated formulations of anticancer agents, Clin. Cancer Res. 11 (2005) 8230–8234.
[9] V. Torchilin, Micellar nanocarriers: pharmaceutical perspectives, Pharm. Res. 24 (2007) 1–16.
[10] X.-X. Zhang, H.S. Eden, X. Chen, Peptides in cancer nanomedicine: drug carriers, targeting ligands and protease substrates, J. Control. Release 159 (2011) 2–13.
[11] S.V. Vinogradov, T.K. Bronich, A.V. Kabanov, Nanosized cationic hydrogels for drug delivery: preparation, properties and interactions with cells, Adv. Drug Deliv. Rev. 54 (2002) 135–147.
[12] M.R. Abidian, D.H. Kim, D.C. Martin, Conducting-polymer nanotubes for controlled drug release, Adv. Mater. 18 (2006) 405–409.
[13] S.-H. Hu, T.-Y. Liu, D.-M. Liu, S.-Y. Chen, Nano-ferrosponges for controlled drug release, J. Control. Release 121 (2007) 181–189.
[14] A.P. Griset, J. Walpole, R. Liu, A. Gaffey, Y.L. Colson, M.W. Grinstaff, Expansile nanoparticles: synthesis, characterization, and *in vivo* efficacy of an acid-responsive polymeric drug delivery system, J. Am. Chem. Soc. 131 (2009) 2469–2471.
[15] G.A. Husseini, G.D. Myrup, W.G. Pitt, D.A. Christensen, N.Y. Rapoport, Factors affecting acoustically triggered release of drugs from polymeric micelles, J. Control. Release 69 (2000) 43–52.
[16] D.E.J.G.J. Dolmans, D. Fukumura, R.K. Jain, Photodynamic therapy for cancer, Nat. Rev. Cancer 3 (2003) 380–387.
[17] K. Park, S. Lee, E. Kang, K. Kim, K. Choi, I.C. Kwon, New generation of multifunctional nanoparticles for cancer imaging and therapy, Adv. Funct. Mater. 19 (2009) 1553–1566.
[18] J. Lu, E. Choi, F. Tamanoi, J.I. Zink, Light-activated nanoimpeller-controlled drug release in cancer cells, Small 4 (2008) 421–426.
[19] J. Babin, M. Pelletier, M. Lepage, J.-F. Allard, D. Morris, Y. Zhao, A new two-photon-sensitive block copolymer nanocarrier, Angew. Chem. Int. Ed. 48 (2009) 3329–3332.
[20] K.L. Kelly, E. Coronado, L.L. Zhao, G.C. Schatz, The optical properties of metal nanoparticles: the Influence of size, shape, and dielectric environment, J. Phys. Chem. B 107 (2003) 668–677.
[21] L. Paasonen, T. Laaksonen, C. Johans, M. Yliperttula, K.S. Kontturi, A. Urtti, Gold nanoparticles enable selective light-induced contents release from liposomes, J. Control. Release 122 (2007) 86–93.
[22] L.J.E. Anderson, E. Hansen, E.Y. Lukianova-Hleb, J.H. Hafner, D.O. Lapotko, Optically guided controlled release from liposomes with tunable plasmonic nanobubbles, J. Control. Release 144 (2010) 151–158.
[23] G. Wu, A. Mikhailovsky, H.A. Khant, C. Fu, W. Chiu, J.A. Zasadzinski, Remotely triggered liposome release by near-infrared light absorption via hollow gold nanoshells, J. Am. Chem. Soc. 130 (2008) 8175–8177.
[24] A.G. Skirtach, C. Dejugnat, D. Braun, A.S. Susha, A.L. Rogach, W.J. Parak, H. Möhwald, G.B. Sukhorukov, The role of metal nanoparticles in remote release of encapsulated materials, Nano Lett. 5 (2005) 1371–1377.
[25] A.G. Skirtach, A. Muñoz Javier, O. Kreft, K. Köhler, A. Piera Alberola, H. Möhwald, W.J. Parak, G.B. Sukhorukov, Laser-induced release of encapsulated materials inside living cells, Angew. Chem. Int. Ed. 45 (2006) 4612–4617.
[26] P. Ghosh, G. Han, M. De, C.K. Kim, V.M. Rotello, Gold nanoparticles in delivery applications, Adv. Drug Deliv. Rev. 60 (2008) 1307–1315.
[27] B. Duncan, C. Kim, V.M. Rotello, Gold nanoparticle platforms as drug and biomacromolecule delivery systems, J. Control. Release 148 (2010) 122–127.
[28] M.C. Daniel, D. Astruc, Gold nanoparticles: assembly, supramolecular chemistry, quantum-size-related properties, and applications toward biology, catalysis, and nanotechnology, Chem. Rev. 104 (2004) 293–346.
[29] E.E. Connor, J. Mwamuka, A. Gole, C.J. Murphy, M.D. Wyatt, Gold nanoparticles are taken up by human cells but do not cause acute cytotoxicity, Small 1 (2005) 325–327.

[30] H. Maeda, The enhanced permeability and retention (EPR) effect in tumor vasculature: the key role of tumor-selective macromolecular drug targeting, Adv. Enzyme Regul. 41 (2001) 189–207.
[31] T. Tanaka, S. Shiramoto, M. Miyashita, Y. Fujishima, Y. Kaneo, Tumor targeting based on the effect of enhanced permeability and retention (EPR) and the mechanism of receptor-mediated endocytosis (RME), Int. J. Pharm. 277 (2004) 39–61.
[32] A.K. Iyer, G. Khaled, J. Fang, H. Maeda, Exploiting the enhanced permeability and retention effect for tumor targeting, Drug Discov. Today 11 (2006) 812–818.
[33] M.S. Yavuz, Y. Cheng, J. Chen, C.M. Cobley, Q. Zhang, M. Rycenga, J. Xie, C. Kim, K.H. Song, A.G. Schwartz, L.V. Wang, Y. Xia, Gold nanocages covered by smart polymers for controlled release with near-infrared light, Nat. Mater. 8 (2009) 935–939.
[34] S.S. Agasti, A. Chompoosor, C.-C. You, P. Ghosh, C.K. Kim, V.M. Rotello, Photoregulated release of caged anticancer drugs from gold nanoparticles, J. Am. Chem. Soc. 131 (2009) 5728–5729.
[35] G. Han, C.-C. You, B.-J. Kim, R.S. Turingan, N.S. Forbes, C.T. Martin, V.M. Rotello, Light-regulated release of DNA and its delivery to nuclei by means of photolabile gold nanoparticles, Angew. Chem. 118 (2006) 3237–3241.
[36] S. Yamashita, Y. Niidome, Y. Katayama, T. Niidome, Photochemical reaction of poly(ethylene glycol) on gold nanorods induced by near infrared pulsed-laser irradiation, Chem. Lett. 38 (2009) 226–227.
[37] F. Thibaudau, Ultrafast photothermal release of DNA from gold nanoparticles, J. Phys. Chem. Lett. 3 (2012) 902–907.
[38] O. Ekici, R.K. Harrison, N.J. Durr, D.S. Eversole, M. Lee, A. Ben-Yakar, Thermal analysis of gold nanorods heated with femtosecond laser pulses, J. Phys. D: Appl. Phys. 41 (2008) 185501.
[39] J. Stehr, C. Hrelescu, R.A. Sperling, G. Raschke, M. Wunderlich, A. Nichtl, D. Heindl, K. Kurzinger, W.J. Parak, T.A. Klar, J. Feldmann, Gold nanostoves for microsecond DNA melting analysis, Nano Lett. 8 (2008) 619–623.
[40] G. Bisker, L. Minai, D. Yelin, Controlled fabrication of gold nanoparticle and fluorescent protein conjugates, Plasmonics (2012), http://dx.doi.org/10.1007/s11468-012-9349-1.
[41] G.B. Braun, A. Pallaoro, G. Wu, D. Missirlis, J.A. Zasadzinski, M. Tirrell, N.O. Reich, Laser-activated gene silencing via gold nanoshell-siRNA conjugates, ACS Nano 3 (2009) 2007–2015.
[42] A. Wijaya, S.B. Schaffer, I.G. Pallares, K. Hamad-Schifferli, Selective release of multiple DNA oligonucleotides from gold nanorods, ACS Nano 3 (2008) 80–86.
[43] P.K. Jain, W. Qian, M.A. El-Sayed, Ultrafast cooling of photoexcited electrons in gold nanoparticle-thiolated DNA conjugates involves the dissociation of the gold-thiol bond, J. Am. Chem. Soc. 128 (2006) 2426–2433.
[44] G. Bisker, D. Yelin, Noble metal nanoparticles and short pulses for nano-manipulations: theoretical analysis, J. Opt. Soc. Am. B 29 (2012) 1383–1393.
[45] S. Lal, S.E. Clare, N.J. Halas, Nanoshell-enabled photothermal cancer therapy: impending clinical impact, Acc. Chem. Res. 41 (2008) 1842–1851.
[46] T.B. Huff, L. Tong, Y. Zhao, M.N. Hansen, J.-X. Cheng, A. Wei, Hyperthermic effects of gold nanorods on tumor cells, Nanomedicine 2 (2007) 125–132.
[47] X. Huang, P. Jain, I. El-Sayed, M. El-Sayed, Plasmonic photothermal therapy (PPTT) using gold nanoparticles, Lasers Med. Sci. 23 (2008) 217–228.
[48] L.C. Kennedy, L.R. Bickford, N.A. Lewinski, A.J. Coughlin, Y. Hu, E.S. Day, J.L. West, R.A. Drezek, A new era for cancer treatment: gold-nanoparticle-mediated thermal therapies, Small 7 (2011) 169–183.
[49] G.S. Terentyuk, G.N. Maslyakova, L.V. Suleymanova, N.G. Khlebtsov, B.N. Khlebtsov, G.G. Akchurin, I.L. Maksimova, V.V. Tuchin, Laser-induced tissue hyperthermia mediated by gold nanoparticles: toward cancer phototherapy, J. Biomed. Opt. 14 (2009) 021016–021019.
[50] B. Van de Broek, N. Devoogdt, A. D'Hollander, H.-L. Gijs, K. Jans, L. Lagae, S. Muyldermans, G. Maes, G. Borghs, Specific cell targeting with nanobody conjugated branched gold nanoparticles for photothermal therapy, ACS Nano 5 (2011) 4319–4328.
[51] I.H. El-Sayed, X. Huang, M.A. El-Sayed, Selective laser photo-thermal therapy of epithelial carcinoma using anti-EGFR antibody conjugated gold nanoparticles, Cancer Lett. 239 (2006) 129–135.
[52] L. Tong, Y. Zhao, T.B. Huff, M.N. Hansen, A. Wei, J.X. Cheng, Gold nanorods mediate tumor cell death by compromising membrane integrity, Adv. Mater. 19 (2007) 3136–3141.
[53] D.P. O'Neal, L.R. Hirsch, N.J. Halas, J.D. Payne, J.L. West, Photo-thermal tumor ablation in mice using near infrared-absorbing nanoparticles, Cancer Lett. 209 (2004) 171–176.
[54] A. Muñoz Javier, P. del Pino, M.F. Bedard, D. Ho, A.G. Skirtach, G.B. Sukhorukov, C. Plank, W.J. Parak, Photoactivated release of cargo from the cavity of polyelectrolyte capsules to the cytosol of cells, Langmuir 24 (2008) 12517–12520.
[55] X. Huang, B. Kang, W. Qian, M.A. Mackey, P.C. Chen, A.K. Oyelere, I.H. El-Sayed, M.A. El-Sayed, Comparative study of photothermolysis of cancer cells with nuclear-targeted or cytoplasm-targeted gold nanospheres: continuous wave or pulsed lasers, J. Biomed. Opt. 15 (2010) 058002.
[56] D.O. Lapotko, E. Lukianova, A.A. Oraevsky, Selective laser nano-thermolysis of human leukemia cells with microbubbles generated around clusters of gold nanoparticles, Lasers Surg. Med. 38 (2006) 631–642.
[57] J. Chen, D. Wang, J. Xi, L. Au, A. Siekkinen, A. Warsen, Z.-Y. Li, H. Zhang, Y. Xia, X. Li, Immuno gold nanocages with tailored optical properties for targeted photothermal destruction of cancer cells, Nano Lett. 7 (2007) 1318–1322.
[58] L. Au, D. Zheng, F. Zhou, Z.-Y. Li, X. Li, Y. Xia, A quantitative study on the photothermal effect of immuno gold nanocages targeted to breast cancer cells, ACS Nano 2 (2008) 1645–1652.
[59] J.-L. Li, M. Gu, Surface plasmonic gold nanorods for enhanced two-photon microscopic imaging and apoptosis induction of cancer cells, Biomaterials 31 (2010) 9492–9498.
[60] L. Minai, D. Yeheskely-Hayon, L. Golan, G. Bisker, E.J. Dann, D. Yelin, Optical nanomanipulations of malignant cells: controlled cell damage and fusion, Small 8 (2012) 1732–1739.
[61] J. You, G. Zhang, C. Li, Exceptionally high payload of doxorubicin in hollow gold nanospheres for near-infrared light-triggered drug release, ACS Nano 4 (2010) 1033–1041.
[62] H. Park, J. Yang, J. Lee, S. Haam, I.-H. Choi, K.-H. Yoo, Multifunctional nanoparticles for combined doxorubicin and photothermal treatments, ACS Nano 3 (2009) 2919–2926.
[63] D. Schrama, R.A. Reisfeld, J.C. Becker, Antibody targeted drugs as cancer therapeutics, Nat. Rev. Drug Discov. 5 (2006) 147–159.
[64] Y. Yarden, M.X. Sliwkowski, Untangling the ErbB signalling network, Nat. Rev. Mol. Cell Biol. 2 (2001) 127–137.
[65] N. Ferrara, Vascular endothelial growth factor: basic science and clinical progress, Endocr. Rev. 25 (2004) 581–611.
[66] S. Li, K.R. Schmitz, P.D. Jeffrey, J.J.W. Wiltzius, P. Kussie, K.M. Ferguson, Structural basis for inhibition of the epidermal growth factor receptor by cetuximab, Cancer Cell 7 (2005) 301–311.
[67] A.J. Grillo-Lopez, C.A. White, C. Varns, D. Shen, A. Wei, A. McClure, B.K. Dallaire, Overview of the clinical development of rituximab: first monoclonal antibody approved for the treatment of lymphoma, Semin. Oncol. 26 (1999) 66–73.
[68] O. Manches, G. Lui, L. Chaperot, R.M. Gressin, J.-P. Molens, M.-C. Jacob, J.-J. Sotto, D. Leroux, J.-C. Bensa, J.L. Plumas, In vitro mechanisms of action of rituximab on primary non-Hodgkin lymphomas, Blood 101 (2003) 949–954.
[69] Harjunpää, Junnikkala, Meri, Rituximab (Anti-CD20) therapy of B-cell lymphomas: direct complement killing is superior to cellular effector mechanisms, Scand. J. Immunol. 51 (2000) 634–641.
[70] D. Shan, J.A. Ledbetter, O.W. Press, Apoptosis of malignant human B cells by ligation of CD20 with monoclonal antibodies, Blood 91 (1998) 1644–1652.
[71] K.C. Grabar, R.G. Freeman, M.B. Hommer, M.J. Natan, Preparation and characterization of Au colloid monolayers, Anal. Chem. 67 (1995) 735–743.
[72] W. Eck, G. Craig, A. Sigdel, G. Ritter, L.J. Old, L. Tang, M.F. Brennan, P.J. Allen, M.D. Mason, PEGylated gold nanoparticles conjugated to monoclonal F19 antibodies as targeted labeling agents for human pancreatic carcinoma tissue, ACS Nano 2 (2008) 2263–2272.
[73] A. Weiss, T.C. Preston, J. Popov, Q. Li, S. Wu, K.C. Chou, H.M. Burt, M.B. Bally, R. Signorell, Selective recognition of rituximab-functionalized gold nanoparticles by lymphoma cells studied with 3D imaging, J. Phys. Chem. C 113 (2009) 20252–20258.
[74] Y. Lu, W.L. Wong, Y.G. Meng, A high throughput electrochemiluminescent cell-binding assay for therapeutic anti-CD20 antibody selection, J. Immunol. Methods 314 (2006) 74–79.
[75] F. Mafuné, J.-Y. Kohno, Y. Takeda, T. Kondow, Dissociation and aggregation of gold nanoparticles under laser irradiation, J. Phys. Chem. B 105 (2001) 9050–9056.
[76] M. Quinten, U. Kreibig, Optical properties of aggregates of small metal particles, Surf. Sci. 172 (1986) 557–577.
[77] O. Warshavski, L. Minai, G. Bisker, D. Yelin, Effect of single femtosecond pulses on gold nanoparticles, J. Phys. Chem. C 115 (2011) 3910–3917.
[78] P. Johnson, M. Glennie, The mechanisms of action of rituximab in the elimination of tumor cells, Semin. Oncol. 30 (2003) 3–8.
[79] A.N. Volkov, C. Sevilla, L.V. Zhigilei, Numerical modeling of short pulse laser interaction with Au nanoparticle surrounded by water, Appl. Surf. Sci. 253 (2007) 6394–6399.
[80] S. Link, C. Burda, B. Nikoobakht, M.A. El-Sayed, Laser-induced shape changes of colloidal gold nanorods using femtosecond and nanosecond laser pulses, J. Phys. Chem. B 104 (2000) 6152–6163.
[81] C.M. Aguirre, C.E. Moran, J.F. Young, N.J. Halas, Laser-induced reshaping of metallodielectric nanoshells under femtosecond and nanosecond plasmon resonant illumination, J. Phys. Chem. B 108 (2004) 7040–7045.
[82] Y. Takeda, F. Mafune, T. Kondow, Selective degradation of proteins by laser irradiation onto gold nanoparticles in solution, J. Phys. Chem. C 113 (2009) 5027–5030.
[83] Y. Takeda, T. Kondow, F. Mafune, Degradation of protein in nanoplasma generated around gold nanoparticles in solution by laser irradiation, J. Phys. Chem. B 110 (2006) 2393–2397.
[84] C. Hrelescu, J. Stehr, M. Ringler, R.A. Sperling, W.J. Parak, T.A. Klar, J. Feldmann, DNA melting in gold nanostove clusters†, J. Phys. Chem. C 114 (2010) 7401–7411.